Nonisothermal Crystallization Kinetics of Isotactic Polypropylene Containing Nucleating Agent and Dispersant

Jun Qin,[1,2] Xiaolang Chen,[3] Jie Yu,[2] Yang Wang,[1] Yaozhu Tian,[2] Song Wu[4]

[1]*Key Laboratory of Karst Environment, Geohazard Prevention (GuizhouUniversity), Ministry of Education, Guiyang 550003, China*
[2]*National Engineering Research Center for Compounding and Modification of Polymer Materials, Guiyang 550014, China*
[3]*Key laboratory of Advanced Materials Technology (Ministry of Education), School of Materials Science and Engineering, Southwest Jiaotong University, Chengdu 610031, China*
[4]*College of Chemical Engineering, Guizhou University, Guiyang 550003, China*

Received 9 January 2009; accepted 6 November 2009
DOI 10.1002/app.31737
Published online 26 March 2010 in Wiley InterScience (www.interscience.wiley.com).

ABSTRACT: In this article, nonisothermal crystallization kinetics was investigated by using differential scanning calorimeter. The Avrami, Ozawa, and combined Avrami with Ozawa (Mo method) equations were applied to describe the crystallization kinetics and estimate the kinetic parameters of mathematical models under the nonisothermal crystallization of isotactic polypropylene (iPP) with rosin nucleating agent (RNA) and calcium stearate as dispersant (CSD). The results show that RNA can improve the crystallization temperature and accelerate the nucleation rate because of its heterogeneous nucleation. The crystal grain sizes of spherulites are smaller for iPP with RNA and CSD together than those for pure iPP and its matrix only filled with RNA. Furthermore, iPP blends with RNA and CSD show a lower Avrami values than that of the pure iPP, and the Mo method can successfully describe the crystallization model under the nonisothermal crystallization. © 2010 Wiley Periodicals, Inc. J Appl Polym Sci 117: 1047–1054, 2010

Key words: polypropylene; nucleation; crystallization; kinetics

INTRODUCTION

It is well known that isotactic polypropylene (iPP) can form large spherulites when it crystallizes from the melt, causing unsatisfactory impact strength, especially at low temperature, and making its products opaque. Several important means have been used in industrial practice to overcome its shortcomings. One of them is adding nucleating agents to vary the crystalline morphology of iPP.

In recent years, the effects of nucleating agents on the crystallization behaviors of PP have been widely investigated.[1–10] These studies showed that the variety and content of nucleating agents had great effect on the degree of crystallinity, crystal size, nucleating rate, and crystal morphology. The researchers[11] found that the nucleation density increased with the addition of 0.8 wt % organic phosphorus nucleating agent, and the crystallization temperature was enhanced by 12 K. Moreover, when 0.4–1.5 wt % sorbitol derivatives were added, the rate of crystallization of PP increased, whereas the surface energy (σ_e) of PP decreased.[12] Hideki et al.[13–15] found that the rosin acid metallic salt could make PP crystallize at a high rate and provide molded articles with excellent mechanical properties and/or optical properties. Compared with other nucleating agents, rosin-type nucleating agent has excellent mechanical and optical properties, odorless products, and cheap. Some patents have already indicated that the crystalline thermoplastic resin with a rosin acid metallic salt and a compatibilizing agent can crystallize at a high rate and have excellent mechanical and optical properties. However, few reports illustrated that alkali dehydroabietate added to PP matrix could greatly increase the rate of crystal nucleation. When rosin-type nucleating agent was added to PP matrix, higher transparency and flexural strength were obtained. It is natural to ask whether there exist synergistic effects on the crystallization of iPP when both the rosin nucleating agent (RNA) and the calcium stearate dispersant (CSD) were added to iPP matrix simultaneously.

Correspondence to: J. Yu (yujiegz@126.com).
Contract grant sponsor: National Key Technology R&D Program; contract grant number: 2007BAB08B05.
Contract grant sponsor: National Science Foundation of Guizhou Province, China; contract grant number: [2005]2096.
Contract grant sponsor: Science and Technology Foundation of Guizhou Province; contract grant number: [2008]7001.

The study of nonisothermal crystallization of polymer is of great technological significance, since most practical processing techniques proceed under nonisothermal conditions. In this work, the nonisothermal crystallization kinetics of the iPP samples in the presence of RNA and/or CSD were investigated by differential scanning calorimetry (DSC). Polarizing light microscopy (PLM) was also used to observe the crystallization morphology. The validity of the modified Avrami equation, Ozawa equation, and Mo method for these systems were discussed in detail.

EXPERIMENTAL

Materials

iPP (injection-molding grade, melting index 15.0 g/10 min ASTM D1238) was provided by Maoming Petrochemial Shihua. The industrial grade RNA and CSD were supplied by Zhejiang Wannn plastics.

iPP (dried at 80°C for 6 h), RNA, CSD, etc., by the recipe were blended in a twin-screw extruder (Type TSE-40A/400-44-22, $L/D = 40$, made in Nanjing, China). The temperatures from hopper to die at six different zones are 170, 180, 190, 200, 210, and 205°C, respectively, and the screw speed is 160 rpm. The extrudates were cut into pellets, and the nucleating iPP samples were prepared. The sample with RNA is marked as PPa, whereas the sample including RNA and CSD is marked as PPb.

Nonisothermal DSC analysis

DSC analysis was performed on a Perkin-Elmer Q 10 under nitrogen flow. The sample of about 8 mg was packed in the aluminum DSC pans and placed in the DSC cell. The samples were heated from 50 to 210°C at a heating rate of 20°C/min and then kept at 210°C for 5 min to eliminate any nuclei that might act as seed crystals. Then, the samples were cooled down to 100°C at cooling rates of 5, 10, 15, and 20°C/min, respectively.

Polarizing light microscopy

A PLM (Nikon E4500) was used to observe the crystal morphology. The samples were first annealed at 210°C for 5 min, and then quickly cooled to 110°C at a cooling rate of 90°C/min. The end images of the crystallization were recorded with an image processor.

RESULTS AND DISCUSSION

Nonisothermal crystallization behaviors

Figure 1 shows nonisothermal crystallization exotherms of pure PP and nucleating PP samples. The onset temperature (T_s), the peak temperature (T_p), and the end temperature (T_e) of the exotherm, and

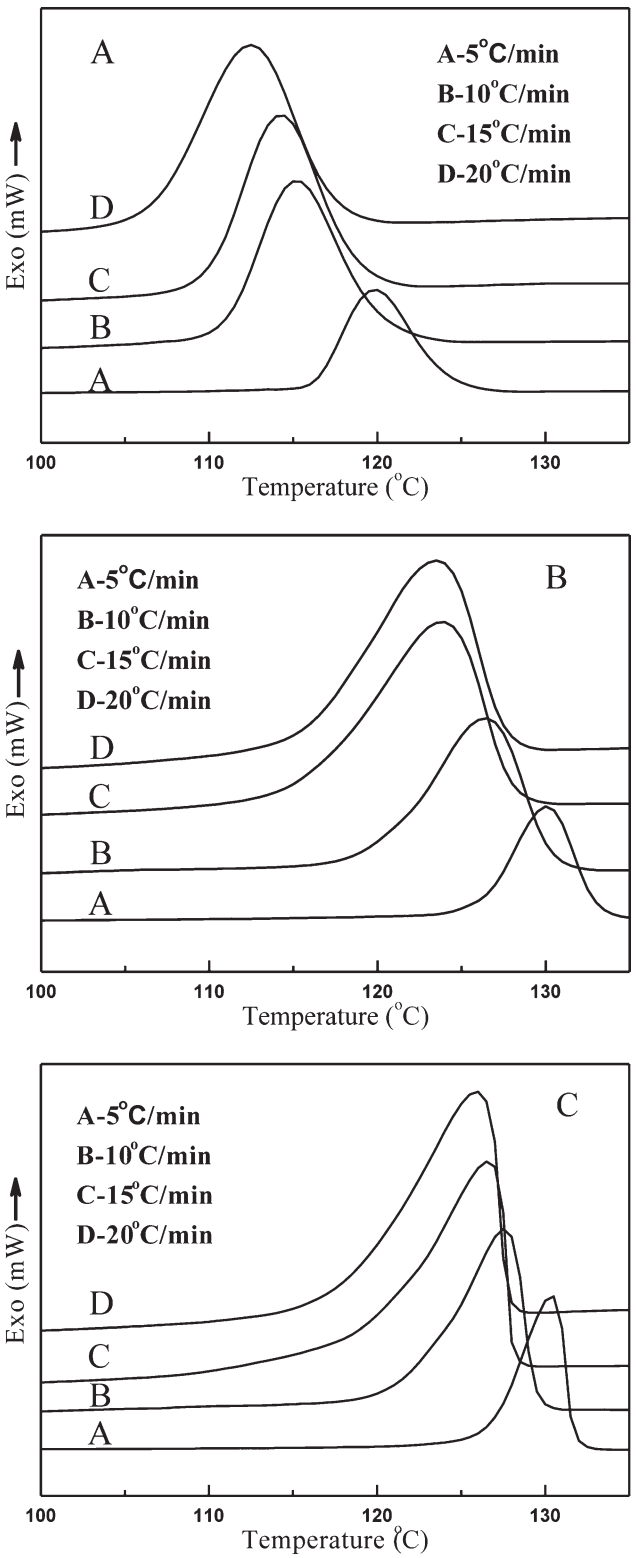

Figure 1 DSC curves of some samples in air at different cooling rates: (A) pure iPP, (B) PPa, and (C) PPb.

the crystallinity degree (X_c) are widely used to describe the nonisothermal crystallization process of polymers.[16,17] The T_s, T_p, T_e, and values of the aforementioned samples are also listed in Table I. As shown in Figure 1, the T_s, T_p, and T_e values of pure

TABLE I
DSC Data on the Rosin Nucleating PP Composites, Obtained from the Cooling DSC Curves

Samples	Cooling rate (°C/min)	T_m^P (°C)	T_s (°C)	T_p (°C)	T_e (°C)	$-H_c$ (J/g)	X_c (%)
Pure iPP	5	164.4	124.2	119.8	116.4	83.4	39.9
	10	163.2	120.2	115.2	110.1	79.8	38.1
	15	164.3	119.0	114.3	109.9	75.8	36.2
	20	165.9	117.4	112.4	106.6	72.6	34.7
PPa	5	166.4	133.0	130.1	126.2	78.3	37.5
	10	166.6	130.4	126.4	120.4	76.9	36.8
	15	165.9	127.9	123.8	116.2	73.1	35.0
	20	167.1	127.5	123.5	115.6	69.6	33.3
PPb	5	166.7	131.6	130.4	126.7	87.2	41.7
	10	166.6	129.4	127.6	122.5	81.5	38.9
	15	166.6	127.9	126.6	120.0	74.7	35.9
	20	166.9	127.7	125.9	119.1	73.6	35.2

PP, PPa, and PPb shift to lower temperature with increasing cooling rate. The current results appear to verify the previous observations[17] that the crystallization peak temperatures increased by about 10–12°C due to the addition of the organic fillers.

There are two major effects acting simultaneously when polymer filled with the organic particles undergoes crystallization. One is the increase in mobility of the chain segments and the other is the heterogeneous nucleation. Increasing in molecular mobility would play a positive effect on the perfect crystallization and the value of T_p would increase. At the same time, the heterogeneous nucleation would accelerate the deposition of polymer molecules, which leads to the increase of T_p.

As shown in Table I, all the T_p values of PPa and PPb are clearly seen to be higher than that of pure PP. Because the rosin is incompatible with PP, the RNA in the PP matrix could more or less hinder the motion of the PP chain segments. This results in producing the smaller and more defects spherulites compared with the homogeneous crystallization of pure PP. At the same time, it can be seen from Table I that a very little amount (0.06 wt %) of calcium stearate would result in increasing polymer chain mobility, and the values of T_p increase. Moreover, with increasing amount of calcium stearate, the heterogeneous nucleation effect will gradually evolve. Providing more sites for nucleation and accelerating the deposition of polymer molecules; the T_p of PPb would shift to higher temperature with the addition of calcium stearate.

X_c, the degree of crystallinity,[18] is defined as following:

$$X_c = \frac{\Delta H_f}{\Delta H_f^0} \tag{1}$$

Where ΔH_f and ΔH_f^0 are the melting enthalpies of PP sample and 100% crystallization PP, respectively, the $\Delta H_f^0 = 209$ J/g.[19] ΔH_f is acquired by the integral area of the heating DSC curve.

Nonisothermal crystallization kinetics

According to the DSC thermograms of nonisothermal crystallization scans, the values of the relative crystallinity at different cooling rates can be determined by the following equation[20]

$$X_t = \frac{\int_{T_0}^{T} (dH_c/dT)dT}{\int_{T_0}^{T_\infty} (dH_c/dT)dT} \tag{2}$$

where T_0 and T_∞ are the onset and end of crystallization temperature, respectively, and dH_c/dT is the heat flow at temperature T. The relative crystallinity of pure PP, PPa, and PPb can be expressed as a function of crystallization time, as shown in Figure 2. It can be seen from Figure 2 that all these curves have the similar sigmoidal shapes, and the curvature of the upper parts of the plot could be due to the spherulite impingement in the later stage of crystallization. The crystallization time (t) can be estimated from the corresponding temperatures by means of[21]

$$t = \frac{T_0 - T}{\alpha} \tag{3}$$

where α is the cooling rate. It seems that the crystallization time of PPb is less to approach the same relative crystallinity at various cooling rates than that of pure iPP and PPa.

Avrami equation

It is well known that the Avrami equation[22,23] can be applied to describe the isothermal crystallization behaviors. Under nonisothermal crystallization, the Avrami equation could still explain the initial stage of crystallization, or the primary crystallization, as follows:

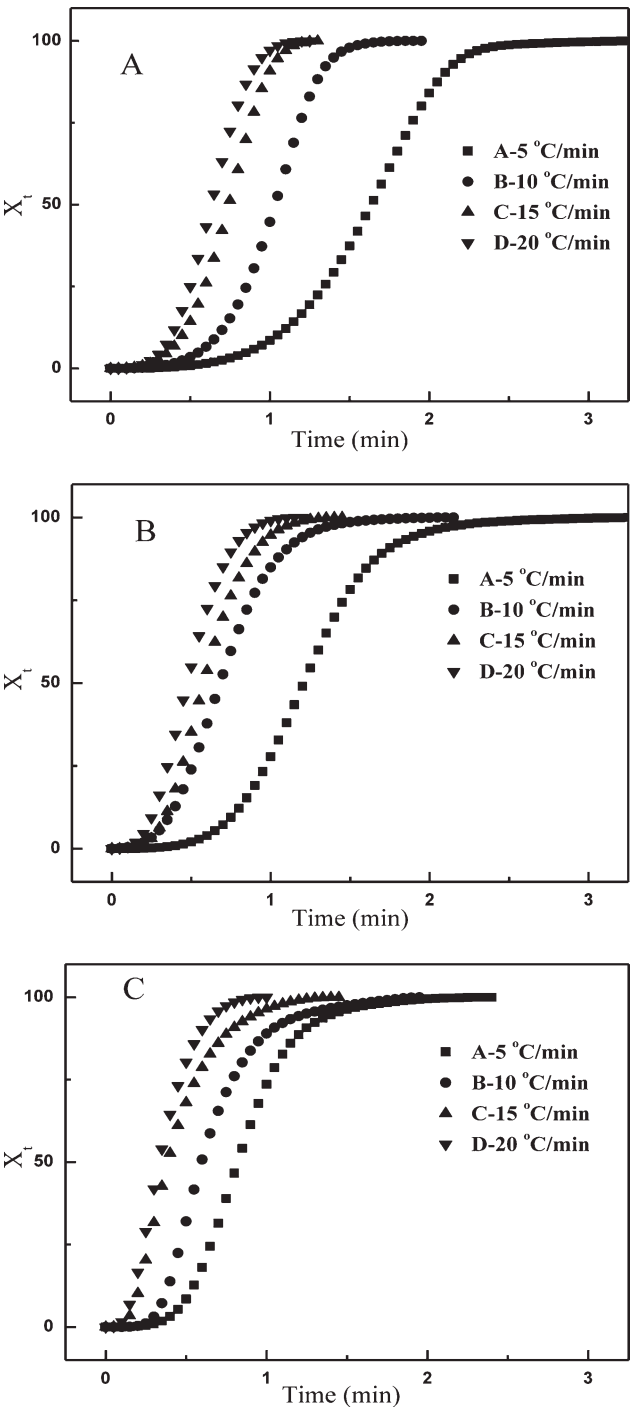

Figure 2 Plots of X_t versus t for crystallization of some samples: (A) pure iPP, (B) PPa, and (C) PPb.

$$1 - X_t = \exp(-Z_t t^n) \quad (4)$$

$$\ln[-\ln(1 - X_t)] = n \ln t + \ln Z_t \quad (5)$$

where X_t is the relative degree of crystallinity at time t. Both the parameter Z_t and the Avrami exponent n are diagnostic of the crystallization mechanism. The parameter of Avrami exponent n describes the growing mechanism and geometry of crystallization, and the parameter Z_c describes the growth rate in the nonisothermal crystallization process. On account of the nonisothermal characteristics of the process investigated, the value of the crystallization rate Z_t should be corrected as[24]

$$\ln Z_c = \frac{\ln Z_t}{\alpha} \quad (6)$$

According to eq. (4), the plot of $\ln[-\ln(1 - X_t)]$ versus $\ln t$ will give the slope n, the Avrami exponent, and the intercept $\ln Z_t$, as shown in Figure 3 and Table II. As shown in Table II, the n values of pure PP are higher than those of RAN or/and CSD filled PP sample, and the value is close to 3, suggesting that nucleation mechanism of pure PP is homogeneous nucleation and three-dimension crystal growth.[1] The crystallization temperature shifts to low temperature while the cooling rates increase. However, this is not accompanied with a lower n value. The possible reason is that the PP crystal grows very fast. Therefore, the more impingement effect, defects spherulites and irregular shape of the spherulites will be produced with increasing cooling rates. Compared with the RNA nucleating PP, the addition of CSD does not lead to a low n value. This indicates that the calcium stearate does not change the nucleation mechanism and the growing geometry of the nucleating PP. All these data show that the nucleation mechanism of PPa and PPb samples are between homogeneous and heterogeneous nucleation.

As expected, the parameter Z_c describes the crystallization rate of the polymer molecules. As shown in Table II, at the same cooling rate, the Z_c values of PPa and PPb are higher than those of pure PP. On account of the relation between the crystallization time t and the crystallization rate Z_c, a lower t value should be accompanied with a higher Z_c value, accounting for the fast crystallization rate. The inclusion of the RNA could hinder the crystallization,[17] and the dispersant offers the more specific area to crystallize under the nonisothermal scans. As a consequence, there are more sites available to nucleate. Each crystal grows to a smaller crystal grain size and cease to grow further, shortening overall crystallization time.[25]

Ozawa equation

The nonisothermal crystallization can be also analyzed by the Ozawa method[18] as follows:

$$\ln[-\ln(1 - X_t)] = \ln K(T) - m \ln \alpha \quad (7)$$

Where $K(T)$ is the crystallization rate constant, X_t is the relative crystallinity, α is the cooling rate, and m

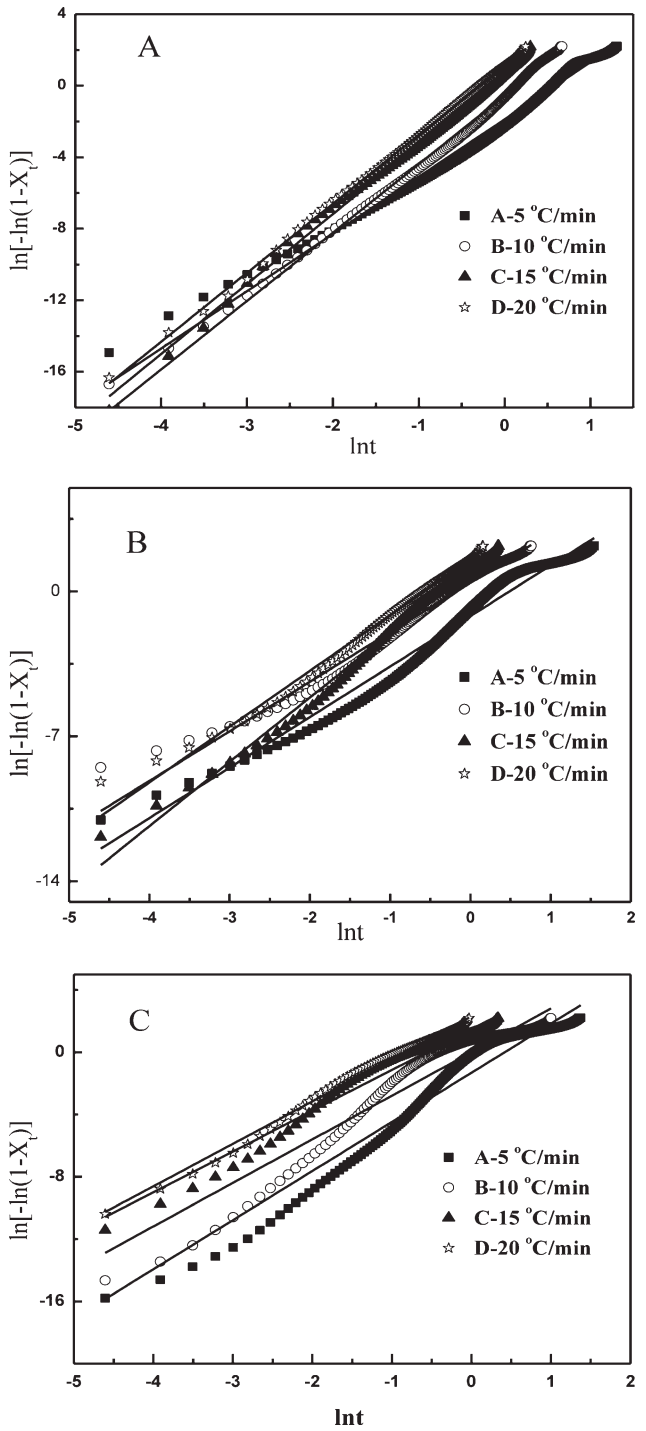

Figure 3 Plots of $\ln[-\ln(1 - X_t)]$ versus $\ln t$ for crystallization of some samples at different cooling rate: (A) pure iPP, (B) PPa, and (C) PPb.

is the Ozawa exponent depending on the crystal growth and nucleation mechanism. Figure 4 shows the nonisothermal crystallization results of several samples according to Ozawa's method. The curvature in Figure 4 prevents an accurate analysis of nonisothermal crystallization data. Under nonisothermal crystallization, the crystallization rate depends on the time and the cooling rate. However, the Ozawa method does not take into account the difference caused by the time and the cooling rate. Some studies have predicted other disregarded factors such as the folded chain length of the polymer chain and the secondary crystallization in the Ozawa method.[26]

The Mo method

A method modified by Mo and coworkers,[27] combining the Avrami equation with the Ozawa equation, was used to describe the nonisothermal crystallization.

$$\ln a = \ln F(T) - b \ln t \tag{8}$$

where $F(T) = [K(T)/Z_t]^{1/m}$ and $b = n/m$. $F(T)$ refers to the necessary value of cooling rate approaching the degree of crystallinity at unit crystallization time. The plots of $\ln a$ versus $\ln t$ for all samples are given in Figure 5, from which the values of b and $F(T)$ can be obtained by the slopes and the intercepts of these lines, respectively (Table III). The $F(T)$ value increases systematically with increasing the relative degree of crystallinity. At a given degree of crystallinity, the higher the $F(T)$ value, the higher cooling rate is needed within unit crystallization time, indicating the difficulty of polymer crystallization. The $F(T)$ values of rosin nucleating PP and rosin/calcium stearate nucleating PP are lower than those of pure PP, indicating that the crystallization rate of PPa and PPb is faster than that of pure iPP. Among those samples, PPa can crystallize easier. This is in accordance with the result obtained from the Avrami approach. The b values of PPb are lower than those of PPa and pure iPP, which indicates that the lower n of PPb is obtained.

TABLE II
The Avrami Exponent n and the Growth Rate Constant Z_c of Crystallization on the PP Composites Under Nonisothermal Crystallization Process

Samples	Cooling rate (°C/min)	n	Z_c (min/°C)
Pure iPP	5	3.20	0.69
	10	3.83	0.95
	15	3.91	1.04
	20	3.85	1.06
PPa	5	2.44	0.79
	10	2.39	1.04
	15	3.10	1.07
	20	2.69	1.08
PPb	5	3.15	0.76
	10	2.79	1.00
	15	2.62	1.10
	20	2.72	1.12

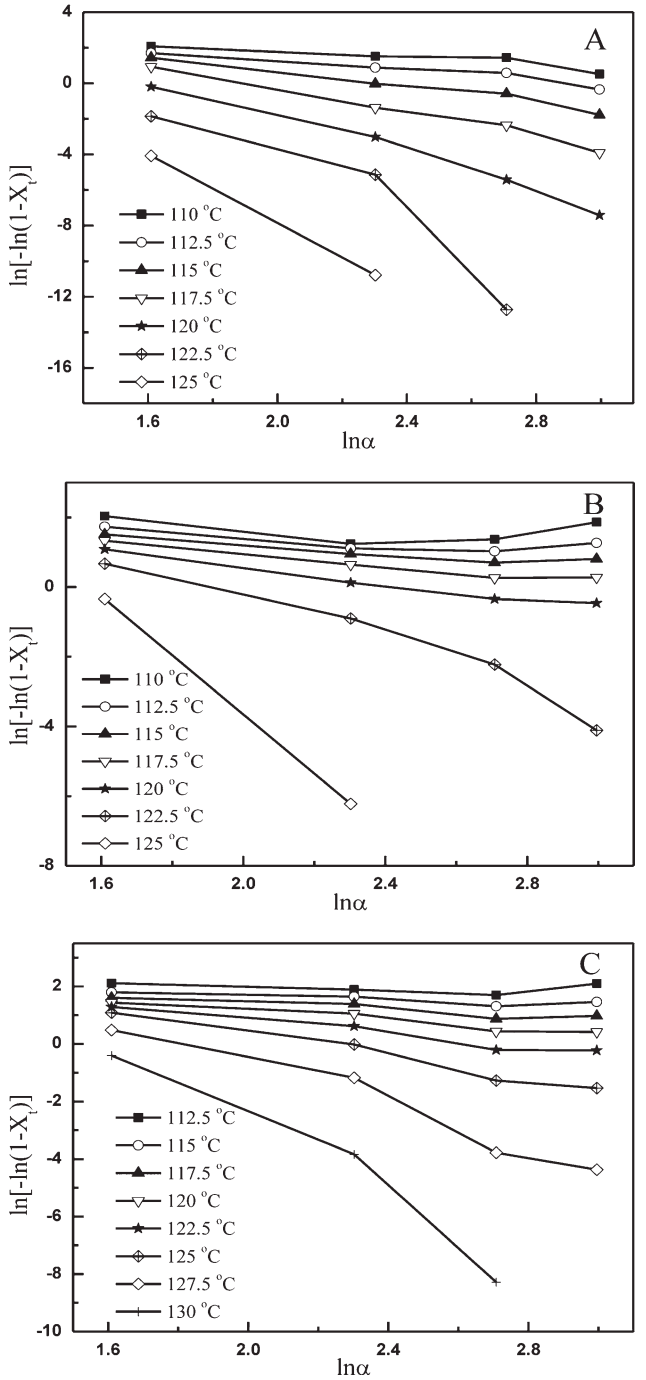

Figure 4 Qzawa plots of ln[−ln(1 − X_t)] versus ln α for nonisothermal crystallization of several samples: (A) pure iPP, (B) PPa, and (C) PPb.

Crystallization activation energy

As for the nonisothermal crystallization at different cooling rates, Kissinger[28] proposed that the crystallization activation energy could be estimated as follows:

$$\frac{\ln(a/T_p^2)}{d(1/T_p)} = \frac{-\Delta E}{R} \tag{9}$$

Accordingly, the crystallization activation energy could be determined from the slope the plot of $\ln(\alpha/T_p^2)$ versus $1/T_p$, as shown in Figure 6 and Table III. The crystallization activation energies of pure PP, rosin nucleating PP, and rosin/calcium stearate nucleating PP are estimated to be 245, 266, and 407 kJ mol^{-1}, respectively. As discussed earlier, RNA and CSD would result in the higher X_c and T_m^p. However, the higher crystallization energy seems to

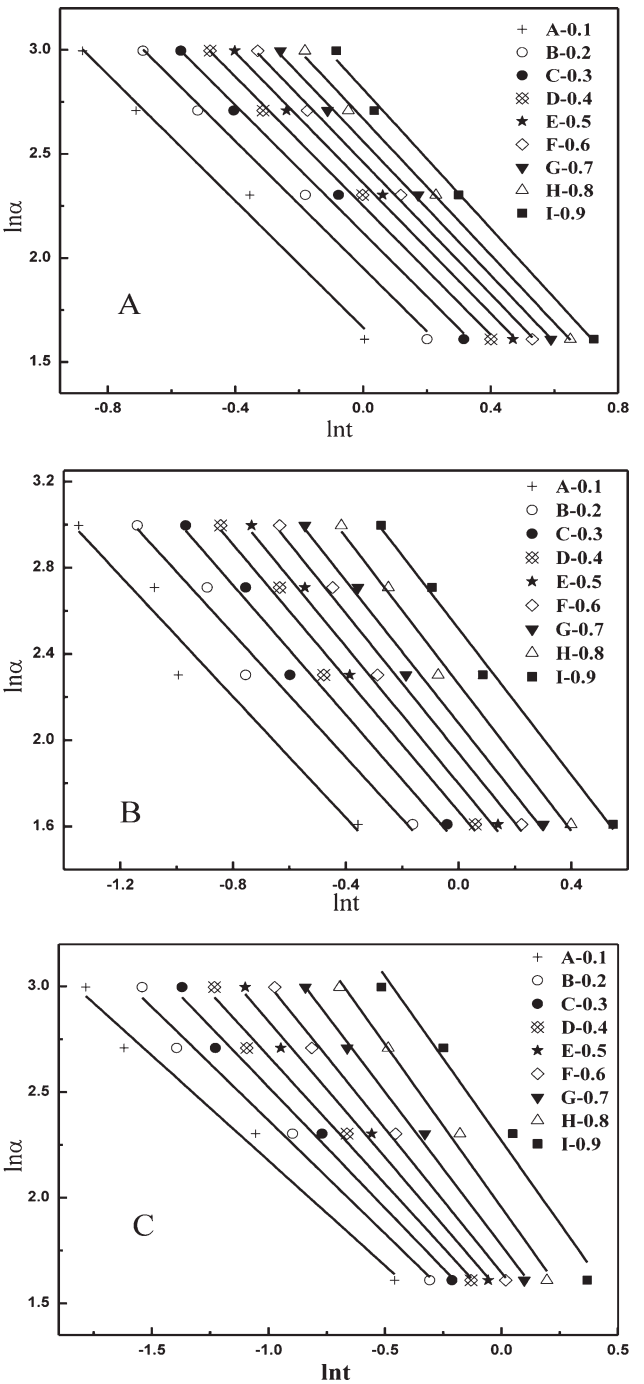

Figure 5 Plots of ln α versus ln t for several samples at each given relative crystallization: (A) pure iPP, (B) PPa, and (C) PPb.

TABLE III
Nonisothermal Crystallization Kinetic Parameters Based on the Mo Method, and the Activation Energy Estimated According to Kissinger Method

Samples	X_t	b	F (K/min)	Activation energy (kJ/mol)
Pure iPP	0.1	1.520	5.294	245
	0.2	1.522	7.048	
	0.3	1.531	8.349	
	0.4	1.549	9.504	
	0.5	1.567	10.602	
	0.6	1.586	11.721	
	0.7	1.609	12.957	
	0.8	1.637	14.445	
	0.9	1.676	16.661	
PPa	0.1	1.403	2.942	266
	0.2	1.433	3.848	
	0.3	1.504	4.554	
	0.4	1.548	5.309	
	0.5	1.590	6.037	
	0.6	1.622	6.954	
	0.7	1.652	7.993	
	0.8	1.705	9.583	
	0.9	1.697	12.386	
PPb	0.1	0.994	3.262	407
	0.2	1.072	3.649	
	0.3	1.145	3.970	
	0.4	1.207	4.319	
	0.5	1.288	4.700	
	0.6	1.364	5.184	
	0.7	1.452	5.897	
	0.8	1.546	7.056	
	0.9	1.560	9.671	

violate the above two influences. The only possibility accounting for this contradiction might be reduced in grain size in the iPP matrix while CSD is introduced.

The crystallization activation energy E_c is also expressed as[29]

$$E_c = (E_N + mE_G)/n \tag{10}$$

where E_N and E_G are the activation energies for nucleation and growth, respectively. The rosin/calcium stearate particles could make the PP molecules easier to nucleation, greatly increase the nucleation rate, the E_N decreases, compared with the rosin nucleated PP, thus the E_G will increase and it will be more difficult to make the composite grow. Obviously, the inclusion of rosin/calcium stearate particles could make the PP molecules easier to nucleate and accelerate the crystallization rates during the dynamic crystallization process, but it also lowers the grain size in the iPP matrix.

PLM observation is used to characterize the crystallization morphology of polymers. Figure 7 shows the crystalline morphologies of pure PP, PPa, and PPb at 110°C. For the pure iPP, the complete spherulite structure is remarkable, the Maltase cross is obvious and the interface of spherulites is clear. While in PPa, a fewer nuclei would be produced because nucleating agent is nonhomodisperse in the iPP Matrix. There are certain amounts of the irregular spherulites produce and remarkably complete spherulites exist, while the interface of spherulites becomes obscure and the Maltase cross is still obvious. In PPb, the incorporation of RNA and CSD can greatly decrease the spherulite size even if CSD content is low. As CSD is introduced, RNA could homodisperse in the iPP matrix to offer more specific area for iPP to crystallize. Because of the existence of a great deal of nuclei, the spherulite cannot grow large enough to overlap due to the very fast nucleation rate and the heterogeneous nucleation followed by a diffusion-controlled growth. Accordingly, the size of spherulites in PPb would be much smaller than those in pure iPP and PPa, and thus no complete spherulite is observed. This accords well with DSC results.

CONCLUSIONS

In this work, the effects of RNA and CSD on crystallization behaviors and nonisothermal crystallization kinetics of iPP were studied. The addition of RNA and CSD has a great effect on the crystallization behaviors of iPP. The Avrami and the Mo method can successfully describe the crystallization behaviors of iPP with RNA and CSD. The heterogeneous nucleation effect depends on the dispersibility of RNA in the iPP matrix. CSD can improve the dispersibility of RNA and reduce the overall crystallization time of RNA nucleated iPP as a result of the combined effects of rapid heterogeneous nucleation and the shorter time to grow to the small final crystal grain size. This factor directly results in the higher crystallization temperature, the smaller crystal grain

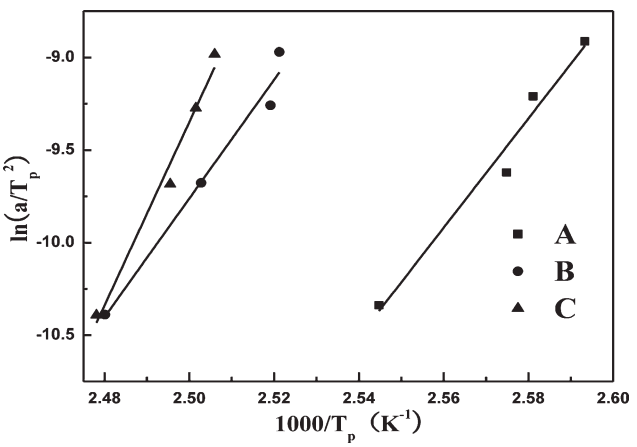

Figure 6 Crystallization activation energies of some samples: (A) pure iPP, (B) PPa, and (C) PPb.

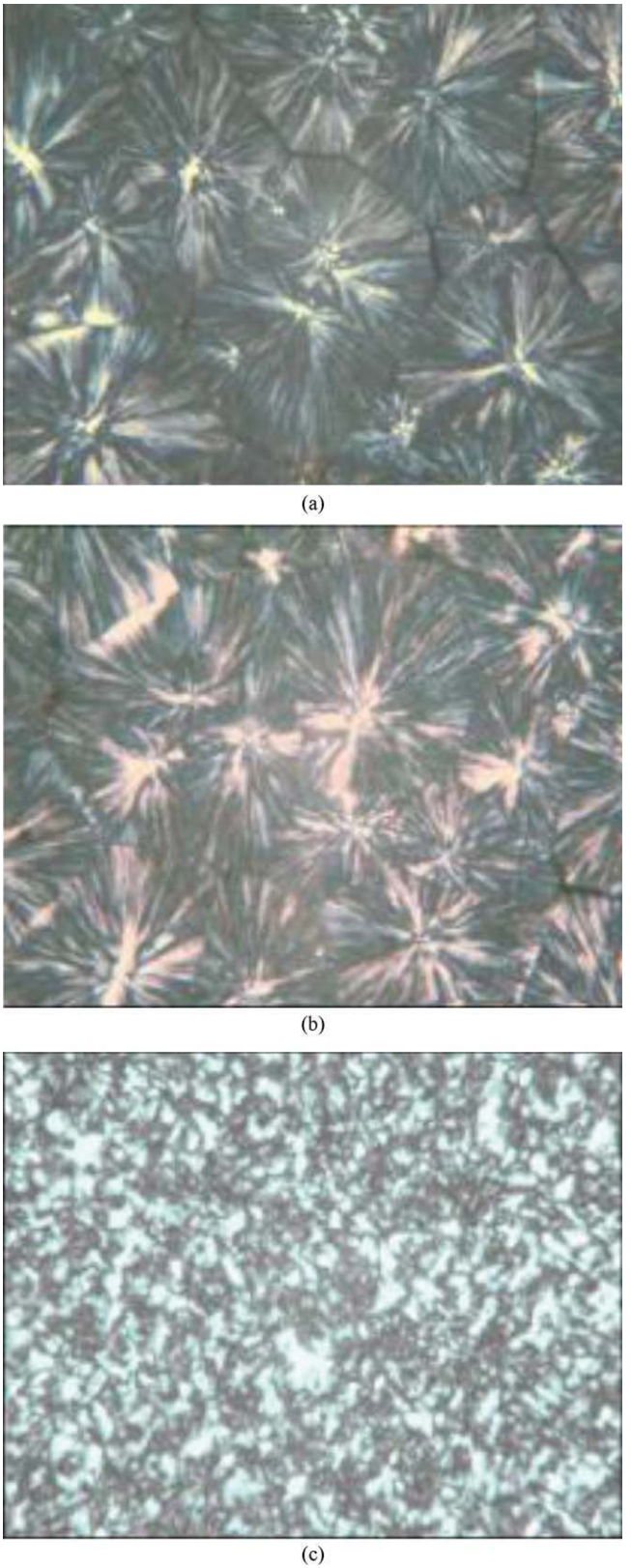

Figure 7 PLM photograph of some samples: (A) pure iPP, (B) PPa, and (C) PPb. [Color figure can be viewed in the online issue, which is available at www.interscience.wiley.com.]

size, the slightly higher crystallinity fraction X_c and T_p, the higher crystallization activation energies, as well as the lower crystallization rate in terms of lower Z_c and $F(T)$. PLM photographs also confirm that there is a correlation among crystallization parameter, the dispersibility of the nucleating agent and the resulting morphologies. The incorporation of RNA and CSD can greatly decrease the spherulite size of iPP, and no complete spherulite of iPP is observed.

References

1. Mubarak, Y.; Harkin-Jones, E. M. A.; Marin, P. J. Polymer 2001, 42, 3171.
2. Valentini, L.; Biagiotti, J.; Lopez-Manchado, M. A.; Santuccis, K. J. M. Polym Eng Sci 2004, 44, 303.
3. Radhakrishnan, S.; Sonawane, P.; Pawaskar, N. J Appl Polym Sci 2004, 92, 615.
4. Oda, T.; Saito, H. J Polym Sci Part B: Polym Phys 2004, 42, 1565.
5. Tjong, S. C.; Chen, S. X.; Li, R. K. Y. J Appl Polym Sci 1997, 64, 707.
6. Kundu, P. P.; Bhattacharya, A. K.; Tripathy, D. K. J Appl Polym Sci 1997, 65, 1759.
7. Lopez-Manchado, M. A.; Arroyo, M. Polymer 1999, 40, 487.
8. Shepard, T. A.; Delsorbo, C. R.; Louth, R. M.; Walborn, J. L.; Norman, D. A.; Harvey, N. G.; Spontak, R. J. J Polym Sci Part B: Polym Phys 1997, 35, 2617.
9. Feng, Y.; Jin, X.; Hay, J. N. J Appl Polym Sci 1998, 69, 2089.
10. Tao, Y. J.; Pan, Y. X.; Zhang, Z. S.; Mai, K. C. Eur Polym J 2008, 44, 1165.
11. Gui, Q. D.; Xin, Z.; Zhu, W. P.; Dai, G. C. J Appl Polym Sci 2003, 88, 297.
12. Zweifel, H. Plastics Additives Handbook, 5th ed.; Hanser: Munich, 2001; p 963.
13. Hideki, S.; Mikio, N.; Tetsuji, K.; Kimio, U.; Masao, M.; Yukiharu, Y.; Hiroyuki, H.; Junji, T.; Kan, M. Eur. Pat. Appl. EP 686,663 Al (1995).
14. Kazumasa, F.; Hitoshi, I. Eur. Pat. Appl. EP 785,231 Al (1997).
15. Takao, T.; Takeshi, O.; Shigenobu, K.; Tatsuo, K. Jpn Kokai Tokkyo Koho JP 10,251,463 A2 (1998).
16. Zhu, G.; Li, C. C.; Li, Z. Y. Eur Polym J 2001, 37, 1007.
17. Chen, X. L.; Yu, J.; Guo, S. Y. J Appl Polym Sci 2006, 102, 4943.
18. Ozawa, T. Polymer 1971, 12, 150.
19. Choudhary, V.; Varma, H. S.; Varma, I. K. Polymer 1991, 32, 2534.
20. Consuelo, R.; Herrero, J. L. Polym J 1994, 26, 786.
21. Kim, S. H.; Ahn, S. H. Polymer 2003, 44, 5625.
22. Xu, X. R.; Xu, J. T.; Chen, L. S.; Liu, R. W.; Feng, L. X. J Appl Polym Sci 2001, 80, 123.
23. Xu, W.; Ge, M.; He, P. J Appl Polym Sci 2001, 82, 2281.
24. Jeziorny, A. Polymer 1978, 19, 1142.
25. Jia, C. M.; Wang, Z. Z.; Liang, X. M.; Hu, Y. Polym Test 2005, 24, 71.
26. Lorenzo, M. L. D.; Silvestre, C. Prog Polym Sci 1999, 24, 917.
27. Liu, T. X.; Mo, Z. S.; Wang, S. G.; Zhang, H. F. Polym Eng Sci 1997, 37, 568.
28. Kissinger, H. E. J Res Natl Stand 1956, 57, 217.
29. Avrami, M. J Chem Phys 1941, 9, 177.